

Triethoxysilane-Catalyzed Single and Sequential Regioselective Hydroboration of Terminal Alkynes: Sustainable Access to *E*-Alkenylboronate and Alkyl *Gem*-Diboronate Esters by Non-Covalent Interactions

Harleen Kaur, Himani Ahuja, and Rebeca Arevalo*


 Cite This: *ACS Catal.* 2025, 15, 976–981


Read Online

ACCESS |

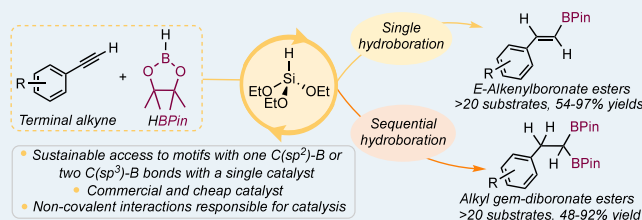
Metrics & More

Article Recommendations

Supporting Information

ABSTRACT: Triethoxysilane was found to be an efficient catalyst for the synthesis of *E*-alkenyl- and alkyl-di-boronate esters by the single and sequential hydroboration of terminal alkynes, respectively, with pinacolborane. Mechanistic studies support that the formation of diboronate esters proceeds by a double hydroboration pathway with the steric and electronic profile at Si being key to enabling the second hydroboration step. Weak non-covalent interactions involving the Si and the C≡C or C=C bonds in the alkynes or alkenylboronate esters have been identified as responsible for substrate activation toward the addition of HBPin.

KEYWORDS: silicon catalysis, sequential hydroboration, non-covalent interactions, terminal alkynes, $C(sp^3)$ -B bonds



INTRODUCTION

Boronate esters with $C(sp^3)$ -B bonds¹ are attractive precursors for the synthesis of drugs² containing 3D non-flat motifs.³ One of the most convenient transformations to access molecular scaffolds with two $C(sp^3)$ -B bonds is the sequential hydroboration of terminal alkynes with pinacolborane (HBPin). Enabling the second hydroboration step remains challenging for main-group⁴ and transition-metal catalysts,⁵ with only three transition-metal complexes⁶ and $(9\text{-BBN})_2$ (9-borabicyclo[3.3.1]nonane dimer, **Scheme 1a**)^{7a} reported efficient for the transformation. The key behind 9-BBN efficiency relies on its ability to add across the multiple C–C bonds of the substrates and promote subsequent trans-borylation steps with HBPin. While neutral silicon catalysis is still in its infancy,⁸ covalent bonding between the perfluorinated strong Lewis acid $\text{Si}(\text{FCat})_2$ (FCat = perfluorocatecholate)⁹ and aldehydes has been reported key for the hydro-silylation of aldehydes (**Scheme 1b**).^{9a} However, weaker non-covalent interactions promoted by weak Lewis acidic Si compounds, such as siloxanes, are unknown to promote additions across multiple bonds. While promising in catalysis,¹⁰ non-covalent interactions are still restricted to the presence of Lewis basic functional groups in the substrates, such as ketones or esters.¹¹

In this work, we report that the neutral, weak Lewis acidic Si compound, HSi(OEt)_3 , is an efficient regio- and stereoselective catalyst for the single and sequential hydroboration of terminal alkynes affording synthetically valuable $\beta\text{-E}$ -alkenylboronate and alkyl *gem*-diboronate esters respectively (**Scheme 1c**). This

work constitutes the first example of sustainable,¹² neutral Si catalysis to construct C–B bonds in hydrocarbons relying on non-covalent interactions to activate multiple C–C bonds.

METHODS

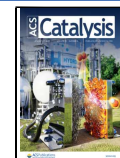
Our research commenced with the assessment of the catalytic efficiency of 30 mol % of HSi(OEt)_3 for the hydroboration of 4-fluorophenylacetylene (**1**) with 3 equiv of HBPin in a 1.0 M solution of 1,4-dioxane at 80 °C for 2 h. Under these conditions, the *E*-alkenylboronate ester **1a** was formed as the exclusive product in an 80% yield (92% conversion of **1**). In contrast, when the reaction was conducted for 24 h under the same conditions, the diboronate ester **1b** was formed as the exclusive product in 84% yield (>99% conversion of **1**). These results support HSi(OEt)_3 as an efficient catalyst for the hydroboration of **1** with HBPin, the time being the determining factor for a single or sequential hydroboration yielding **1a** or **1b**, respectively. Control experiments supported the need of HSi(OEt)_3 to access **1a** and **1b** in a synthetically useful yield (pp S10–S12 in the SI). For both processes, reactions on the gram-scale were conducted under the optimized conditions shown in **Scheme 2a** and **b** (see Tables

Received: November 6, 2024

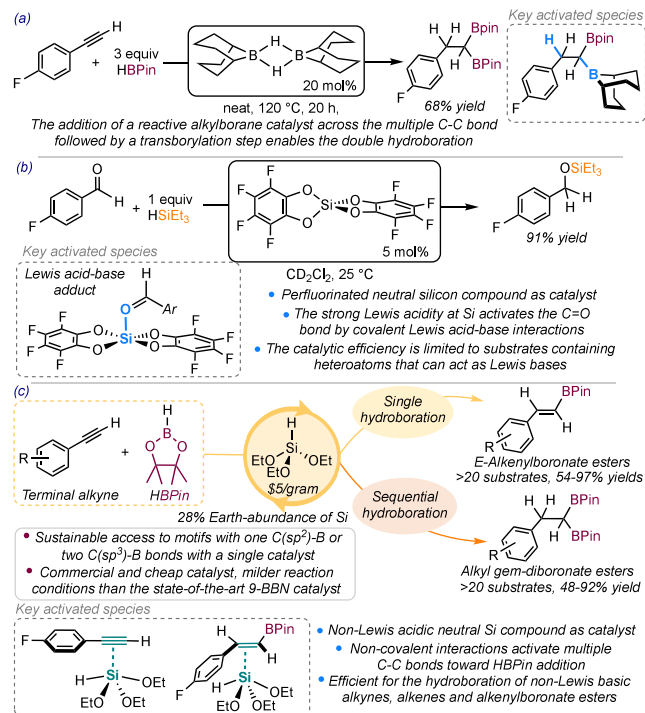
Revised: December 25, 2024

Accepted: December 30, 2024

Published: January 1, 2025



Scheme 1. Main-Group Catalysis for the Hydrofunctionalization of Multiple Bonds and Key Activated Species^a



^a(a) Sequential hydroboration of 4-fluorophenylacetylene with HBPin catalyzed by 9-BBN;^{7a} (b) hydrosilylation of aldehydes catalyzed by a neutral Si compound;^{9a} and (c) this work: HSi(OEt)₃-catalyzed single and sequential hydroboration of terminal alkynes enabled by non-covalent interactions.

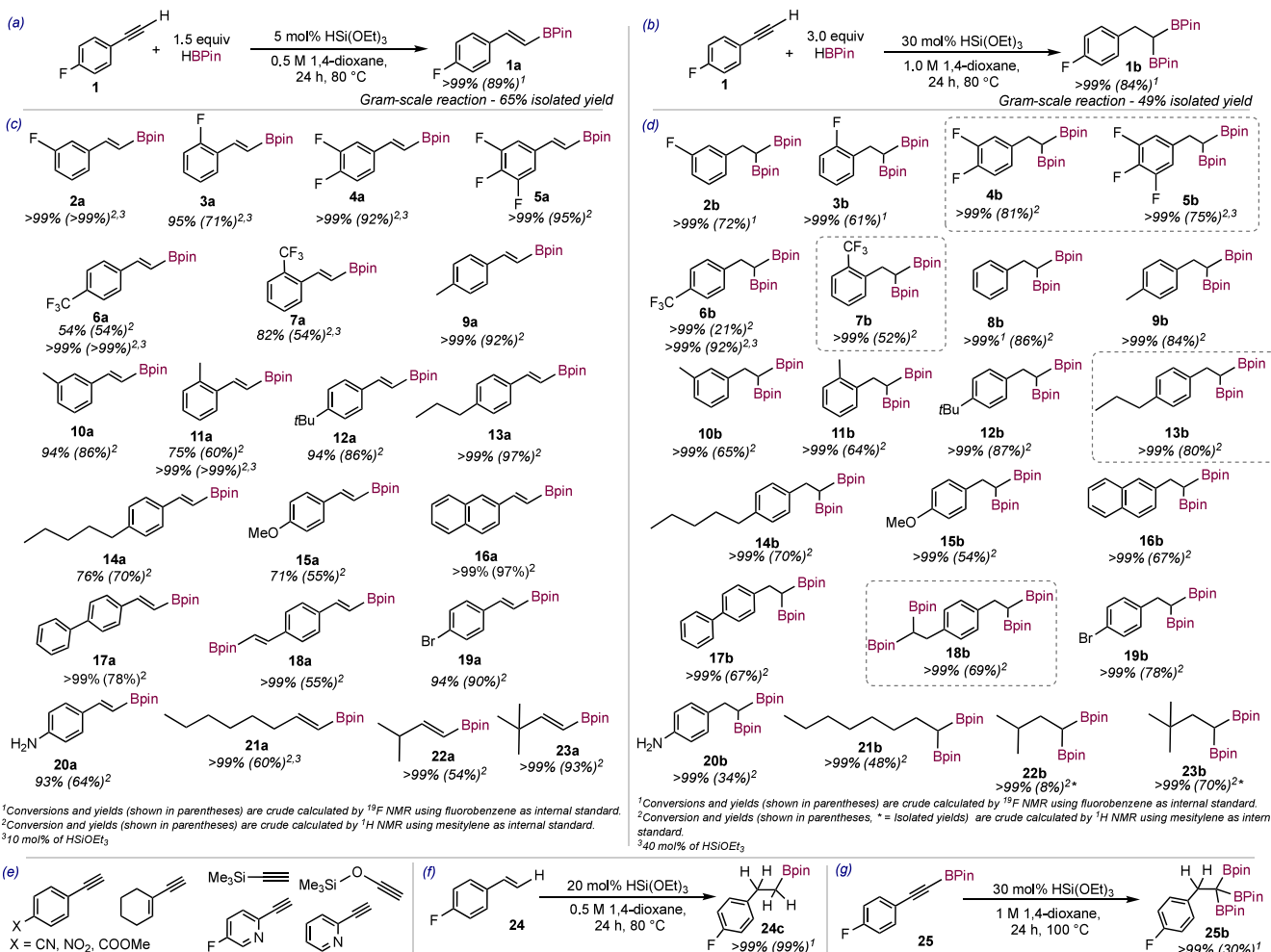
S3 and S4 in the SI for the full optimization of conditions) and the substrate scope was explored (Scheme 2c and d). Aromatic alkynes with electron-withdrawing groups afforded products in lower yields than those with electron-donating alkyl groups (e.g., 54% for **6a** and 92% for **9a**) suggesting that increased electronic density at the aryl ring resulted in more efficient catalysis. However, substituents at the *ortho* position of the aryl ring led to decreased product yields (e.g., 60% for **11a** and 92% for **9a**), hinting that increased steric hindrance at the C≡C bond resulted in decreased catalyst efficiency. Polyfluorinated aromatic alkynes **4**, **5**, and **7**¹³ as well as **13** and the dialkyne **18** were efficiently hydroborated for the first time, affording novel boronate esters (**4b**, **5b**, **7b**, **13b**, and **18b** respectively, boxed in gray in Scheme 2d). HSi(OEt)₃ was also efficient for the aliphatic alkynes **21–23** and for the single hydroboration of 4-fluorostyrene (**24**, Scheme 2f), the sequential hydroboration of the alkynylboronate **25** (Scheme 2g),¹⁴ and the single hydroboration of **1** with HBCat (Cat = catecholate, product **1c** in p S6 in the SI), and was found inefficient for the hydroboration of the alkynes depicted in Scheme 3e (p S45 in the SI). Control experiments employing BH₃–THF as the precatalyst and trapping BH₃ experiments (pp S12–S17 in the SI) ruled out hidden-boron catalysis¹⁵ as responsible for observed yields of **1a** and **1b**; however, BH₃ formed at late stages of the reaction could contribute to a minor extent (<11%) to the yield of **1b**. The synthetic approach described here presents significant advantages over the reported Sc(OTf)₃¹⁶ and 9-BBN^{7a} catalysts for the single and sequential hydroboration of terminal alkynes respectively,

mainly the milder temperature and lower catalyst loadings in the absence of a strong hydride source as *in situ* activator.¹⁶ Furthermore, unlike Sc(OTf)₃ and 9-BBN,^{7a} HSi(OEt)₃ is capable of accessing both, alkenyl- and alkyldiboronate esters, under the appropriate conditions.

To elucidate the keys behind catalyst efficiency, the hydroboration of **1** with 3 equiv of HBPin in the presence of 50 mol % of HSi(OEt)₃ in THF-*d*₈ at 80 °C was monitored by ¹H, ¹⁹F, ¹¹B, ¹³C, and ²⁹Si NMR spectroscopy. The ¹⁹F and ¹H NMR spectra showed the conversion of **1** (at -110.7 ppm in the ¹⁹F NMR spectrum) into **1a** (at -112.8 ppm in the ¹⁹F NMR spectrum) and of **1a** into **1b** (at -118.9 ppm in the ¹⁹F NMR spectrum; p S47 in the SI), supporting two operative sequential hydroboration cycles (Schemes 3a and b). Independent monitoring of the hydroboration of **1a** further supported the formation of **1b** from **1a** (pp S64–S69 in the SI). The fluorinated analog HSi(OCH₂CF₃)₃¹⁷ was found more efficient for the transformation (pp S57–S58 in the SI), as evidenced by the times required to reach 92% conversion of **1** (2 h and 5 min) and 51% conversion of **1a** (10 h and 30 min), shorter than those when HSi(OEt)₃ was employed (4 h 30 min and 14 h 30 min, respectively, Scheme 3b). Furthermore, the times required for the formation of **1b** are longer than those for **1a**, suggesting slower turnover for the second cycle and/or loss of catalyst efficiency over time. In both cases, signals attributable to H₂ (4.50 ppm) in the ¹H NMR spectra and to a mixture of products containing B (broad signals at 22.14 (major) and 35.00 ppm (minor) in the ¹¹B NMR spectra) and Si (-68.55, -40.01, -42.49 ppm in the ²⁹Si NMR spectra) were observed, the intensity of which grew over time. The signal at 22.14 ppm in the ¹¹B NMR spectra was attributed to O(BPin)₂ based on the ¹¹B and ¹³C NMR spectra. The NMR monitoring of the reaction of HSi(OEt)₃ with 1 equiv of HBPin showed the same signals (pp S76–S79 in the SI) supporting reactions involving these species taking place during catalysis. The addition of an equimolar mixture of **1** and HBPin to the isolated mixture of species and heating at 80 °C for 24 h resulted in recovery of the starting materials, supporting the side reactions involving HBPin and HSi(OEt)₃ as deactivation pathways that could result in decreased catalyst efficiency over time.

The ¹H NMR spectra of the catalytic reaction did not show any changes in the multiplicity of the signals attributed to **1**, **1a**, and HSi(OEt)₃, suggesting that covalent bonding between the substrates and HSi(OEt)₃, including the addition of the Si–H bond across the multiple bonds of **1** or **1a**,^{7a} did not take place during catalysis. However, the signals attributed to **1**, **1a**, and HSi(OEt)₃ shifted from those of samples of the individual reagents in the ¹H, ¹³C, and ²⁹Si NMR spectra throughout catalysis (e.g., ¹H $\Delta\delta$ ¹⁸ (HSi(OEt)₃) = +0.013 ppm; ¹³C $\Delta\delta$ (C2 in **1**) = +0.066 ppm upon mixing the reagents and $\Delta\delta$ (C2 in **1a**) = +0.012 ppm at 21% conversion of **1a**, see Scheme 3a for labeling scheme; and ²⁹Si $\Delta\delta$ (HSi(OEt)₃) = -0.062 ppm upon mixing the reagents and -0.244 ppm at 21% conversion of **1a**, see Table S8 in the SI). The shift of the signals suggests that non-covalent interactions between HSi(OEt)₃ and **1** or **1a** are present during the catalytic reaction. The direction of the shifts, downfield for the C2 in **1** and **1a** and upfield for the Si in HSi(OEt)₃, suggest that the non-covalent interactions increase the electronic density on the Si and deplete that of the C≡C and C=C bonds in **1** and **1a**, respectively, facilitating the addition of HBPin.

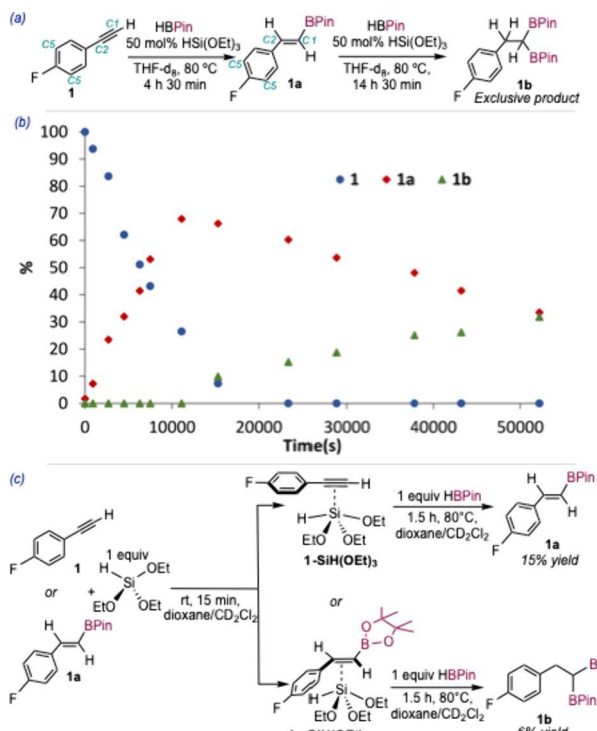
Scheme 2. (a) Single and **(b)** Sequential Hydroboration of 4-Fluorophenylacetylene with HBPin Catalyzed by HSi(OEt_3) under Optimized Conditions to Access **(a)** *E*-Alkenylboronate and **(b)** Alkyldiboronate Esters, Including the Syntheses of **1a** and **1b** on the Gram Scale; Substrate Scope for the **(c)** Single Hydroboration and **(d)** Sequential Hydroboration (New Molecules Are Boxed in Grey); **(e)** Substrates for Which HSi(OEt_3) Was Inefficient (see p S45 in the **SI**); **(f)** Single Hydroboration of 4-Fluorostyrene under Optimized Conditions and **(g)** Sequential Hydroboration of 4-Fluorophenylalkynylboronate Ester under Nonoptimized Conditions



To gain some insights into plausible intermediates in the catalytic cycle, stoichiometric reactions between the components of the catalytic system were conducted (Scheme 3c). The addition of 1 equiv of HSi(OEt_3 to dioxane/CD₂Cl₂ (12:1) solutions of **1** or **1a** at room temperature resulted in an immediate upfield shift of the signal attributable to HSi(OEt_3 in the ²⁹Si NMR spectra ($\Delta\delta^{29}$ (HSi(OEt_3) = -0.026 and -0.053 ppm for the mixtures with **1** and **1a**, respectively) concomitant with downfield shifts of the signals attributed to **1** (e.g., $\Delta\delta$ (C2 in **1**) = +0.213 ppm) or **1a** ($\Delta\delta$ (C2 in **1a**) = +0.276 ppm), respectively, in the ¹³C NMR spectra (Tables S13 and S14 in the **SI**), in the same direction as those observed during the catalytic reaction. For both **1** and **1a**, the ¹³C NMR $\Delta\delta$ for the aryl C atoms (e.g., $\Delta\delta$ (C5 in **1**) = +0.053 ppm and $\Delta\delta$ (C5 in **1a**) = +0.067 ppm) were smaller than those of C1 (+0.741 ppm for **1**) and C2 (+0.213 ppm for **1** and +0.276 ppm for **1a**) engaged in the C≡C and C=C bonds of **1** and **1a**, respectively. This observation points toward the interactions of **1** and **1a** with HSi(OEt_3 taking place mostly through the multiple C–C bonds. Titration experiments involving the addition of increasing amounts of HSi(OEt_3

to CD₂Cl₂ solutions of **1** or **1a** showed analogous shifts of the signals, further supporting non-covalent interactions between the catalyst and the substrates (pp S69–S75 in the **SI**). Based on these observations, plausible adducts present in solutions of HSi(OEt_3 and **1** (**1**-SiH(OEt)₃) or **1a** (**1a**-SiH(OEt)₃) are depicted in Scheme 3c (see p S92 in the **SI** for other plausible adducts in equilibrium). The addition of 1 equiv of HBPin to the **1a**-SiH(OEt)₃ solution resulted in additional shifts of the signals attributed to **1a**-SiH(OEt)₃ and HBPin in the ¹³C NMR spectrum, as well as of that of the Si in the ²⁹Si NMR spectrum (pp S84–S87 in the **SI**), suggesting that HBPin interacted with the **1a**-SiH(OEt)₃ adduct. Heating the solutions of **1a**-SiH(OEt)₃ and of **1**-SiH(OEt)₃ after the addition of HBPin at 80 °C for 1.5 h resulted in the formation of products **1a** and **1b** respectively (Scheme 3c), supporting the adducts as catalytically competent. The adduct obtained by the addition of 1 equiv of HBPin to a HSi(OEt_3 (1 equiv) solution showed analogous results upon the addition of **1a** (pp S88–S91 in the **SI**), suggesting that interaction of any of the substrates, HBPin, **1**, or **1a**, with HSi(OEt_3 can lead to catalytically active adducts.

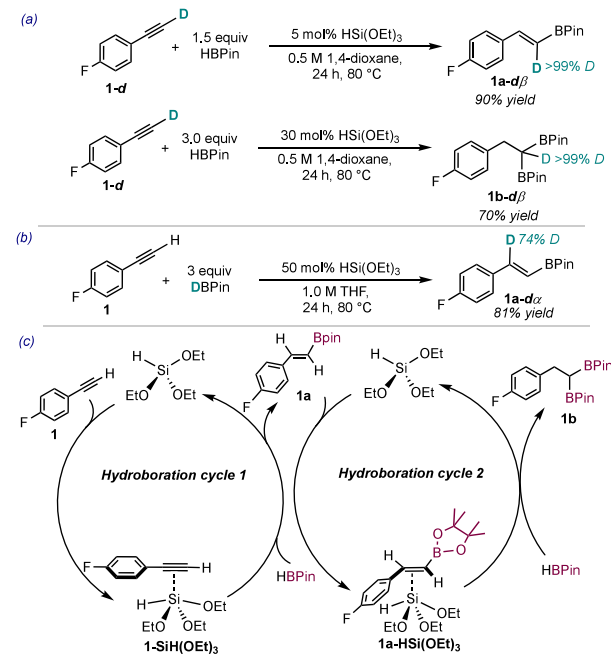
Scheme 3. (a) Reaction Pathway for the HSi(OEt_3)-Catalyzed Sequential Hydroboration of Terminal Alkynes; (b) Quantitative Reaction Profile; (c) Stoichiometric Reactions Supporting the Presence of Non-Covalent Interactions in Catalysis



The increased efficiency of HSi(OEt_3 for alkynes with electron-donating substituents at the *para* position as well as the increased efficiency of $\text{HSi(OCH}_2\text{CF}_3)_3$ suggest that electron-rich substrates with low steric hindrance, or a more electron-deficient catalyst, render adducts with stronger catalyst–substrate interactions, resulting in an increased C–C bond activation toward the addition of HBPin. Additionally, when 1 equiv of OPEt₃ or pyridine was added to the catalytic reaction, **1b** was not detected and **1a** was formed in lower yields than under the optimized catalytic conditions (pp S26–S27 in the SI), suggesting that Lewis bases compete with **1** and **1a** to engage in interactions with HSi(OEt_3 , leading to decreased catalyst efficiency. Lower product yields were also obtained when the strong Lewis acids SiCl_4 or BF_3OEt_2 were employed as catalysts (pp S25–S26 in the SI), highlighting that the weak Lewis acidic HSi(OEt_3 and $\text{HSi(OCH}_2\text{CF}_3)_3$ ²⁰ override the efficiency of strong Lewis acids for this transformation. Furthermore, the catalytic efficiency for the sequential hydroboration was unique to HSi(OEt_3 , as evidenced by the diminished or lack of efficiency of other commercial silicon compounds such as HSi(OiPr_3 (p S18 in the SI), which was capable of engaging in non-covalent interactions with **1a** (see p S74 in the SI for titration experiments) but did not render product **1b** under catalytic conditions.

Deuterium-labeling experiments employing **1-d** as starting material resulted in the formation of products **1a-d β** and **1b-d β** in analogous yields to those of **1a** and **1b** and with >99% D incorporation (Scheme 4a), supporting that C(sp)–H bond activation of **1** does not take place during catalysis.²¹ When the catalytic reaction was conducted employing a 1.05 M solution

Scheme 4. Deuterium Labelling Experiments Employing **1-d for the Single (a, Top) and Sequential (a, Bottom) Hydroboration and DBPin (b), and (c) Proposed Catalytic Cycle**



of DBPin in THF under the conditions optimized for the formation of **1b**, only **1a-d α** was formed in 81% yield (Scheme 4b), suggesting that the cleavage of the D–B bond hinders the formation of **1a** and **1b**.²² NMR monitoring of the reaction of DBPin and HSi(OEt_3 supported that H/D exchange took place under the catalytic reaction conditions after 15 min (p S22 in the SI), accounting for the <99% D incorporation observed in **1a-d α** (Scheme 4b).

Based on the results presented, catalytic cycles that account for the formation of **1a** and **1b** by the HSi(OEt_3 -catalyzed hydroboration of **1** are depicted in Scheme 4c. In both cycles, HSi(OEt_3 enters the cycles by interaction of **1** or **1a** to afford the **1-SiH(OEt)₃** and **1a-SiH(OEt)₃** adducts, respectively, which promote the H–B bond cleavage of HBPin and its addition across the C≡C and C=C bonds, yielding products **1a** and **1b**, respectively.

CONCLUSION

In conclusion, HSi(OEt_3 was found to be an efficient catalyst for the single and sequential hydroboration of alkynes showing a wide substrate scope. Mechanistic experiments supported non-covalent interactions between the multiple C–C bonds of the alkyne or the alkenylboronate ester and the Si atom in HSi(OEt_3 as responsible for their activation toward the addition of HBPin.

ASSOCIATED CONTENT

Supporting Information

The Supporting Information is available free of charge at <https://pubs.acs.org/doi/10.1021/acscatal.4c06845>.

Complete experimental details, characterization data, NMR spectroscopic data (PDF)

AUTHOR INFORMATION

Corresponding Author

Rebeca Arevalo – Department of Chemistry and Biochemistry, University of California—Merced, Merced, California 95343, United States;  orcid.org/0000-0003-4085-6770; Email: rebecaarevalo@ucmerced.edu

Authors

Harleen Kaur – Department of Chemistry and Biochemistry, University of California—Merced, Merced, California 95343, United States

Himani Ahuja – Department of Chemistry and Biochemistry, University of California—Merced, Merced, California 95343, United States

Complete contact information is available at:
<https://pubs.acs.org/10.1021/acscatal.4c06845>

Author Contributions

R.A. conceived the project, designed the experiments, supervised the experimental work, and drafted the manuscript. H.K. conducted the optimization of the reaction conditions, the control experiments, the evaluation of the substrate scope for the single hydroboration of alkynes, the single hydroboration of 4-fluorostyrene, the double hydroboration of the alkynylboronate ester, and the mechanistic studies and drafted the SI and the manuscript. H.A. conducted the evaluation of the substrate scope for the double hydroboration of alkynes and the hydroboration experiments employing strong Lewis acids and in the presence of Lewis bases and drafted the SI. H.K. and H.A. conducted the experiments for the manuscript revisions. The manuscript was written through contributions of all authors. All authors have given approval to the final version of the manuscript.

Funding

University of California, Merced, start-up funds for Rebeca Arevalo.

Notes

The authors declare no competing financial interest.

ACKNOWLEDGMENTS

R.A., H.K., and H.A. thank the ACS PRF for a DNI grant. R.A. thanks the NSF for an MPS-LEAPS grant and Prof. Julio Perez for insightful scientific discussions and his invaluable mentorship.

DEDICATION

Dedicated to the memory of Prof. Julio Perez.

REFERENCES

- (a) Liskey, C. W.; Hartwig, J. F. Iridium-Catalyzed Borylation of Secondary C–H Bonds in Cyclic Ethers. *J. Am. Chem. Soc.* **2012**, *134*, 12422–12425. (b) Ohmura, T.; Torigoe, T.; Suginome, M. Iridium-Catalyzed Borylation of Sterically Hindered C(sp³)–H Bonds: Remarkable Rate Acceleration by a Catalytic Amount of Potassium Tert-Butoxide. *Chem. Commun.* **2014**, *50*, 6333–6336. (c) Liskey, C. W.; Hartwig, J. F. Iridium-Catalyzed C–H Borylation of Cyclopropanes. *J. Am. Chem. Soc.* **2013**, *135*, 3375–3378. (d) Kawazu, R.; Torigoe, T.; Kuninobu, Y. Iridium-Catalyzed C(sp³)–H Borylation Using Silyl-Bipyridine Pincer Ligands. *Angew. Chem., Int. Ed.* **2022**, *61*, No. e202202327. (e) Wang, Y.; Li, Y.; Wang, L.; Ding, S.; Song, L.; Zhang, X.; Wu, Y.-D.; Sun, J. Ir-Catalyzed Regioselective Dihydroboration of Thioalkynes Toward Gem-Diboryl Thioethers. *J. Am. Chem. Soc.* **2023**, *145*, 2305–2314. (f) Park, S. Recent Advances in Catalytic Dearomatic Hydroboration of N-Heteroaromatics. *ChemCatChem.* **2020**, *12*, 3170–3185. (g) Wang, R.; Park, S. Rhodium-Catalyzed Double Hydroboration of Quinolines. *ACS Catal.* **2023**, *13*, 7067–7078. (h) Oeschger, R.; Su, B.; Ehinger, C.; Yu, I.; Romero, E. A.; He, S.; Hartwig, J. F. Diverse Functionalization of Strong, Alkyl C–H Bonds by Undirected Borylation. *Science* **2020**, *368*, 736–741.
- (2) (a) Ma, X.; Kuang, Z.; Song, Q. Recent Advances in the Construction of Fluorinated Organoboron Compounds. *JACS Au* **2022**, *2*, 261–279. (b) Jayaraman, R.; Kireilis, T.; Eriksson, L.; Szabo, K. J. Asymmetric Organocatalytic Homologation: Access to Diverse Chiral Trifluoromethyl Organoboron Species. *Chem.—Eur. J.* **2022**, *28*, No. e202202059. (c) Douglas, J. J.; Adams, B. W. V.; Benson, H.; Broberg, K.; Gillespie, P. M.; Hoult, O.; Ibraheem, A. K.; Janbon, S.; Janin, G.; Parsons, C. D.; Sigerson, R. C.; Klauber, D. J. Multikilogram-Scale Preparation of AZD4635 via C–H Borylation and Bromination: The Corrosion of Tantalum by a Bromine/Methanol Mixture. *Org. Process Res. Dev.* **2019**, *23*, 62–68. (d) Geier, S. J.; Vogels, C. M.; Westcott, S. A. Boron Reagents in Synthesis. ACS Symposium Series; In Coca, A., Ed.; American Chemical Society: Washington, DC, 2016; Vol. 1236, pp 209–225. (e) Fyfe, J. W. B.; Watson, A. J. B. Recent developments in organoboron chemistry: old dog, new tricks. *Chem.* **2017**, *3*, 31–55. (f) Namirembe, S.; Morken, J. P. Reactions of organoboron compounds enabled by catalyst-promoted metalate shifts. *Chem. Soc. Rev.* **2019**, *48*, 3464. (g) Miyaura, N.; Suzuki, A. Palladium-Catalyzed Cross-Coupling Reactions of Organoboron Compounds. *Chem. Rev.* **1995**, *95*, 2457–2483.
- (3) (a) Lovering, F.; Bikker, J.; Humblet, C. Escape from Flatland: Increasing Saturation as an Approach to Improving Clinical Success. *J. Med. Chem.* **2009**, *52*, 6752–6756. (b) Brown, N. Bioisosteres and Scaffold Hopping in Medicinal Chemistry. *Mol. Inf.* **2014**, *33*, 458–462. (c) Mykhailiuk, P. K. Saturated bioisosteres of benzene: where to go next? *Org. Biomol. Chem.* **2019**, *17*, 2839–2849.
- (4) (a) Magre, M.; Maity, B.; Falconet, A.; Cavallo, L.; Rueping, M. Magnesium-Catalyzed Hydroboration of Terminal and Internal Alkynes. *Angew. Chem., Int. Ed.* **2019**, *58*, 7025–7029. (b) Bismuto, A.; Thomas, S. P.; Cowley, M. J. Aluminum Hydride Catalyzed Hydroboration of Alkynes. *Angew. Chem., Int. Ed.* **2016**, *55*, 15356–15359. (c) Fleige, M.; Mobus, J.; vom Stein, T.; Glorius, F.; Stephan, D. W. Lewis Acid Catalysis: Catalytic Hydroboration of Alkynes Initiated by Piers' Borane. *Chem. Commun.* **2016**, *52*, 10830–10833. (d) Magre, M.; Szewczyk, M.; Rueping, M. S-Block Metal Catalysts for the Hydroboration of Unsaturated Bonds. *Chem. Rev.* **2022**, *122*, 8261–8312. (e) Bhandari, M.; Kaur, M.; Rawat, S.; Singh, S. Hydroboration of Imines and Alkynes Catalyzed by Electronically Unsaturated Aluminum Hydride and Methyl Aluminum Cations. *Inorg. Chem.* **2023**, *62*, 6598–6607. (f) Nagao, K.; Yamazaki, A.; Ohmiya, H.; Sawamura, M. Phosphine-Catalyzed Anti-Hydroboration of Internal Alkynes. *Org. Lett.* **2018**, *20*, 1861–1865.
- (5) (a) Geier, S. J.; Vogels, C. M.; Melanson, J. A.; Westcott, S. A. The transition metal-catalysed hydroboration reaction. *Chem. Soc. Rev.* **2022**, *51*, 8877–8922. (b) Bose, S. K.; Mao, L.; Kuehn, L.; Radius, U.; Nekvinda, J.; Santos, W. L.; Westcott, S. A.; Steel, P. G.; Marder, T. B. First-Row d-Block Element-Catalyzed Carbon–Boron Bond Formation and Related Processes. *Chem. Rev.* **2021**, *121*, 13238–13341. (c) Obligacion, J. V.; Chirik, P. J. Earth-Abundant Transition Metal Catalysts for Alkene Hydrosilylation and Hydroboration: Opportunities and Assessments. *Nat. Rev. Chem.* **2018**, *2*, 15–34. (d) Singh, A.; Shafiei-Haghghi, S.; Smith, C. R.; Unruh, D. K.; Findlater, M. Hydroboration of Alkenes and Alkynes Employing Earth-Abundant Metal Catalysts. *Asian J. Org. Chem.* **2020**, *9*, 416–420. (e) Yoshida, H. Borylation of Alkynes underBase/Coinage Metal Catalysis: Some Recent Developments. *ACS Catal.* **2016**, *6*, 1799–1811. (f) Duran Arroyo, V.; Arevalo, R. Tandem Manganese Catalysis for the Chemo-, Regio-, and Stereoselective Hydroboration of Terminal Alkynes: In Situ Precatalyst Activation Led to Enhanced Chemoselectivity. *RSC Adv.* **2024**, *14*, 5514–5523.
- (6) (a) Zuo, Z.; Huang, Z. Synthesis of 1,1-diborionate esters by cobalt catalyzed sequential hydroboration of terminal alkynes. *Org.*

Chem. Front. **2016**, *3*, 434–438. (b) Lee, S.; Li, D.; Yun, Y. Copper-Catalyzed Synthesis of 1,1-Diborylalkanes through Regioselective Dihydroboration of Terminal Alkynes. *Chem.—Asian J.* **2014**, *9*, 2440–2443. (c) Endo, K.; Hirokami, M.; Shibata, T. Synthesis of 1,1-Organodiboronates via Rh(I)Cl-Catalyzed Sequential Regioselective Hydroboration of 1-Alkynes. *Synlett* **2009**, *2009*, 1331–1335.

(7) (a) Docherty, J. H.; Nicholson, K.; Dominey, A. P.; Thomas, S. P. A Boron-Boron Double Transborylation Strategy for the Synthesis of Gem-Diborylalkanes. *ACS Catal.* **2020**, *10*, 4686–4691 For a main-group catalyst for the sequential hydroboration of alkynylboronate esters, see: (b) Doan, S. H.; Mai, B. K.; Nguyen, T. V. A Universal Organocatalyst for Selective Mono-, Di-, and Triboration of Terminal Alkynes. *ACS Catal.* **2023**, *13*, 8099–8105.

(8) (a) Sugiura, M.; Kotani, S.; Nakajima, M. Chapter 11: Catalysis by Silicon Species. In *Catalysis with Earth-Abundant Elements*; Scheneider, U., Thomas, S. P., Eds.; Royal Society of Chemistry, 2020. (b) Ansmann, N.; Thorwart, T.; Greb, L. Silicon Catalyzed C–O Bond Ring Closing Metathesis of Polyethers. *Angew. Chem., Int. Ed.* **2022**, *61*, No. e202210132. (c) Bisai, M. K.; Pahar, S.; Das, T.; Vanka, K.; Sen, S. S. Transition Metal Free Catalytic Hydroboration of Aldehydes and Aldimines by Amidinato Silane. *Dalton Trans.* **2017**, *46*, 2420–2424.

(9) (a) Liberman-Martin, A. L.; Bergman, R. G.; Tilley, T. D. Lewis Acidity of Bis(perfluorocatecholato)silane: Aldehyde Hydrosilylation Catalyzed by a Neutral Silicon Compound. *J. Am. Chem. Soc.* **2015**, *137*, 5328–5331. (b) Maskey, R.; Schädler, M.; Legler, C.; Greb, L. Bis(perchlorocatecholato)silane—A Neutral Silicon Lewis Super Acid. *Angew. Chem., Int. Ed.* **2018**, *57*, 1717–1720.

(10) (a) Mahmudov, K. T.; Pombeiro, A. J. L. Control of Selectivity in Homogeneous Catalysis through Noncovalent Interactions. *Chem.—Eur. J.* **2023**, *29*, No. e202203861. (b) Wang, D. W.; Li, X.; Zhou, P. P.; Wang, Y. Catalysis with Supramolecular Carbon-Bonding Interactions. *Angew. Chem., Int. Ed.* **2021**, *60*, 22717–22721. (c) Jovanovic, D.; Poliyodath Mohanan, M.; Huber, S. M. Halogen, Chalcogen, Pnictogen, and Tetrel Bonding in Non-Covalent Organocatalysis: An Update. *Angew. Chem., Int. Ed.* **2024**, *63*, No. e202404823. (d) Tong, Q.; Zhao, Z.; Wang, Y. A Se–O bonding catalysis approach to the synthesis of calix[4]pyrroles. *Beilstein J. Org. Chem.* **2022**, *18*, 325–330. (e) Zhou, B.; Gabbai, F. P. Anion Chelation via Double Chalcogen Bonding: The Case of a Bis-telluronium Dication and Its Application in Electrophilic Catalysis via Metal-Chloride Bond Activation. *J. Am. Chem. Soc.* **2021**, *143*, 8625–8630.

(11) (a) Zhao, Z.; Pang, Y.; Zhao, Z.; Zhou, P.-P.; Wang, Y. Supramolecular catalysis with ethers enabled by dual chalcogen bonding activation. *Nat. Commun.* **2023**, *14*, 6347. (b) Zhao, Z.; Liu, Y.; Wang, Y. Weak Interaction Activates Esters: Reconciling Catalytic Activity and Turnover Contradiction by Tailored Chalcogen Bonding. *J. Am. Chem. Soc.* **2024**, *146*, 13296–13305. (c) Jain, S.; Thorat, R. A.; Shinu, S. P. P.; Chaurasia, D.; Kumar, S. Tellurium empowered catalysis for enantioselective seleno-michael addition reaction. *ChemRxiv* **2024**, DOI: 10.26434/chemrxiv-2024-h40w6.

(12) Si is the second most abundant element in the Earth-crust (28% of abundance), see: Lide, D. R. *CRC Handbook of Chemistry and Physics*, 89th ed.; CRC Press: Boca Raton, FL, 2008; section 4, p 1.

(13) Due to the ubiquitous presence of fluorinated motifs in drugs, these new molecules could be the key to advance drug discovery. See references **3a**, **b**, and: (a) Inoue, M.; Sumii, Y.; Shibata, N. Contribution of Organofluorine Compounds to Pharmaceuticals. *ACS Omega* **2020**, *5*, 10633–10640. (b) Purser, S.; Moore, P. R.; Swallow, S.; Gouverneur, V. Fluorine in Medicinal Chemistry. *Chem. Soc. Rev.* **2008**, *37*, 320–330. (c) Gouverneur, V.; Seppelt, K. Introduction: Fluorine Chemistry. *Chem. Rev.* **2015**, *115*, 563–565. (d) Müller, K.; Faeh, C.; Diederich, F. Fluorine in Pharmaceuticals: Looking Beyond Intuition. *Science* **2007**, *317*, 1881–1886. (e) O'Hagan, D. Fluorine in health care: Organofluorine containing blockbuster drugs. *J. Fluorine Chem.* **2010**, *131*, 1071–1081. (f) He, J.; Li, Z.; Dhawan, G.; Zhang, W.; Sorochinsky, A. E.; Butler, G.; Soloshonok, V. A.; Han, J. Fluorine-containing drugs approved by

the FDA in 2021. *Chin. Chem. Lett.* **2023**, *34*, 107578. (g) Chandra, G.; Singh, D. V.; Mahato, G. K.; Patel, S. Fluorine—a Small Magic Bullet Atom in the Drug Development: Perspective to FDA Approved and COVID-19 Recommended Drugs. *Chem. Zvesti* **2023**, *1*–22. (h) Shabir, G.; Saeed, A.; Zahid, W.; Naseer, F.; Riaz, Z.; Khalil, N.; Muneeba; Albericio, F. Chemistry and Pharmacology of Fluorinated Drugs Approved by the FDA (2016–2022). *Pharmaceuticals* **2023**, *16*, 1162. (i) O'Hagan, D.; Young, R. J. Future challenges and opportunities with fluorine in drugs? *Med. Chem. Res.* **2023**, *32*, 1231–1234.

(14) For applications of triboronate esters, see: (a) Palmer, W. N.; Zarate, C.; Chirik, P. J. Benzyltriboronates: Building Blocks for Diastereoselective Carbon–Carbon Bond Formation. *J. Am. Chem. Soc.* **2017**, *139*, 2589–2592. (b) Lee, B.; Chirik, P. J. Ketone Synthesis from Benzylboronates and Esters: Leveraging α -Boryl Carbanions for Carbon–Carbon Bond Formation. *J. Am. Chem. Soc.* **2020**, *142*, 2429–2437.

(15) (a) Macleod, J.; Bage, A. D.; Meyer, L. M.; Thomas, S. P. Hidden Boron Catalysis: A Cautionary Tale on TMEDA Inhibition. *Org. Lett.* **2024**, *26*, 9564–9567. (b) Uzelac, M.; Yuan, K.; Ingleson, M. J. A Comparison of Two Zinc Hydride Catalysts for Terminal Alkyne C–H Borylation/Hydroboration and the Formation of 1,1,1-Triborylalkanes by Tandem Catalysis Using Zn–H and B–H Compounds. *Organometallics* **2020**, *39*, 1332–1338. (c) Bage, A. D.; Hunt, T. A.; Thomas, S. P. Hidden Boron Catalysis: Nucleophile-Promoted Decomposition of HBpin. *Org. Lett.* **2020**, *22*, 4107–4112. (d) Bage, A. D.; Nicholson, K.; Hunt, T. A.; Langer, T.; Thomas, S. P. The Hidden Role of Boranes and Borohydrides in Hydroboration Catalysis. *ACS Catal.* **2020**, *10*, 13479–13486.

(16) Mandal, S.; Verma, P. K.; Geetharani, K. Lewis Acid Catalysis: Regioselective Hydroboration of Alkynes and Alkenes Promoted by Scandium Triflate. *Chem. Commun.* **2018**, *54*, 13690–13693.

(17) Synthesized according to the procedure described in: Muramatsu, W.; Manthena, C.; Nakashima, E.; Yamamoto, H. Peptide Bond-Forming Reaction via Amino Acid Silyl Esters: New Catalytic Reactivity of an Aminosilane. *ACS Catal.* **2020**, *10*, 9594–9603.

(18) For the catalytic reaction, the $\Delta\delta$'s were calculated as follows: $\Delta\delta = \delta$ ([signal attributed to atom] in [reagent] in the catalytic reaction) – δ ([signal attributed to atom] in [reagent] in an independent sample containing only the reagent). All the spectra were recorded in THF-*d*₈ at 23 °C.

(19) For the stoichiometric reactions, the $\Delta\delta$'s were calculated as follows: $\Delta\delta = \delta$ ([signal attributed to atom] in [reagent] in the stoichiometric reaction) – δ ([signal attributed to atom] in [reagent] in an independent sample containing only the reagent). All the spectra were recorded in THF-*d*₈ at 23 °C.

(20) ³¹P NMR $\Delta\delta$ (POEt₃) was –0.01 ppm for HSi(OEt)₃ and +0.07 ppm for HSi(OCH₂CF₃)₃, significantly lower than that reported in reference **9a** for Si(^FCat)₂ (+35.9). Assessed by the Gutmann–Beckett method (see pp S24–S25 in the SI for a full description).

(21) A C–H borylation/semihydrogenation pathway could lead to the products from hydroboration, and it has been previously reported operative for the hydroboration of terminal alkynes with HBPin catalyzed by manganese complexes, see reference **5f**.

(22) When the reaction was conducted for 72 h, a mixture of **1a-d α** and **1b-d α** along with other unidentified products was obtained (see p S23 in the SI).